NANO LETTERS

2007
Vol. 7, No. 8
2263−2266

# Label-Free Optical Detection and Tracking of Single Virions Bound to Their Receptors in Supported Membrane Bilayers

**Helge Ewers,[†] Volker Jacobsen,[‡] Enrico Klotzsch,[‡] Alicia E. Smith,[†] Ari Helenius,[†] and Vahid Sandoghdar*[,‡]**

*Institute of Biochemistry, ETH Zurich, CH-8093 Zurich, Switzerland, and Nano-Optics Group, Laboratory of Physical Chemistry, ETH Zurich, CH-8093 Zurich, Switzerland*

*Received April 2, 2007*

**ABSTRACT**

**We apply an interferometric optical detection scheme to image and track unlabeled single virions. Individual simian virus 40 virions and uninfectious virus-like particles were imaged on a glass substrate and on a supported membrane bilayer. Moreover, single unlabeled virions were tracked when bound to supported membrane bilayers via the viral receptor, the glycolipid GM1. The technology presented here promises to be generally applicable to studying the motion of unlabeled macromolecules on membranes.**

The past decade has witnessed a renewed interest in optical imaging for biological investigations. This has been in part triggered by the possibility of detecting single fluorescent molecules and their use as nanoscopic optical labels. Indeed, many well-controlled biophysical studies have exploited this technique, for example for studying the motions of individual viruses[1] or molecular motors.[2] Single molecule fluorescence experiments are, however, confronted with the problem of photobleaching, which limits imaging times to tens of seconds.[3] Recently a few groups have proposed to circumvent this issue by promoting gold nanoparticles as optical labels of unlimited photostability.[4−8] One of the methods used for the detection of particles down to a diameter of 5 nm has been based on the interferometric measurement of particle scattering.[4,6] Interestingly, we have found that this method can be also used to directly detect biological entities such as microtubules without the need for any labeling.[6] Furthermore, optical interferometry has been recently applied to record the passage of individual 100 nm viruses[9] in a flow chamber as bursts and to detect tobacco mosaic viruses using a near-field microscope.[10] However, tracking experiments or time-resolved measurements of biologically relevant parameters such as the diffusion constant of a nanoscopic particle have not been reported yet using this technique. Here we show that it is possible to detect and track single unlabeled small virions attached to their receptors in supported membrane bilayers under aqueous buffer.

Simian virus 40 (SV40) is a small (45 nm diameter), DNA tumor virus from the polyomavirus family, whose human members JC- and BK-viruses are associated with cancer and lethal diseases. The virion is not enveloped by a membrane but has an outer protein shell consisting mainly of 360 copies of the VP1 protein arranged in 72 pentamers around a ∼5000 base-pair genome. The structure of the virion is solved[11] and the cellular receptor was identified as the lipid GM1.[12] The VP1 protein pentamers in the SV40 capsid bind to the pentasaccharide head group of the sphingolipid GM1. By binding to GM1, SV40 induces local signaling in the cellular membrane before internalization into the cell, leading to infection.[13,14] How the virus induces signaling by binding to a lipid that is confined to the outer leaflet of the plasma membrane bilayer is not well understood. The SV40−GM1 interaction is thus of special current interest in medicine and biology.

As described in detail in refs 4, 6, and 15, our method is based on the interference between the light scattered by a nanoparticle and a reference beam, which in our case is the reflection of the incident laser beam from the substrate surface. For very small signals, the contrast becomes proportional to the particle polarizability $\alpha$ and is thus about 16 times smaller for a spherical particle with a refractive index of $n = 1.5$ than for a gold sphere of the same diameter at the wavelength of 532 nm.[4,6,15] Considering that the mass of a virus is largely dominated by protein (>85% for SV40)

* To whom correspondence may be addressed: E-mail: vahid.sandoghdar@ethz.ch.
[†] Institute of Biochemistry, ETH Zurich.
[‡] Nano-Optics Group, Laboratory of Physical Chemistry, ETH Zurich.

10.1021/nl070766y CCC: $37.00 
**Published on Web 07/18/2007**

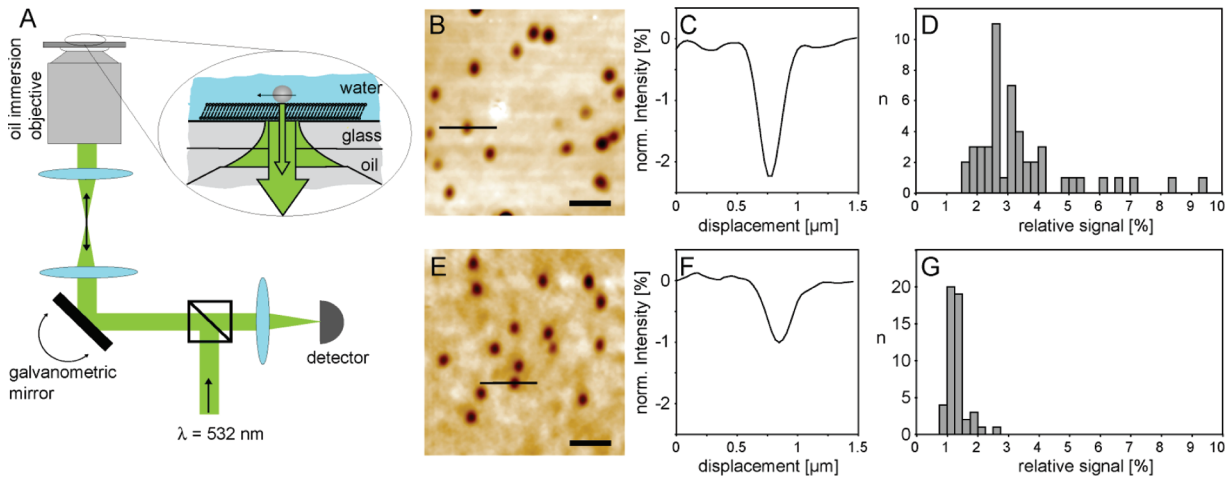


**Figure 1.** Label-free detection of individual SV40 virions and virus-like particles by an interferometric optical microscopy scheme: (A) microscopy setup used; (B) scanning interferometric image of SV40 virions on cover glass; (C) intensity cross section of a single particle; (D) distribution of signal intensities; (E) scanning interferometric image of SV40 virus-like particles; (F) intensity cross section of individual virus-like particle; (G) distribution of the corresponding signal intensities. Scale bar is 1 $\mu$m.

and that $n$ has been measured to be about 1.5 for proteins,[16] we use the $D^3$ scaling law of $\alpha$ and the data in ref 6 to estimate that a virus with a diameter of 45 nm in aqueous medium would result in a signal contrast of about 2.6%.

SV40 virions and virus-like particles were produced and purified as described in refs 14 and 17. Dilute virions in aqueous buffer were added to plasma cleaned cover glass on the stage of a custom-built microscope as depicted in Figure 1A. To detect the scattering from virions at the glass−water interface, a laser beam at the wavelength of 532 nm was scanned over the sample via galvanometric mirrors. The reflected light was collected with an oil immersion objective (100×, NA = 1.4, Zeiss), passed through a beam splitter, and focused by a 200 mm lens on a photodiode (S6058, Hamamatsu). Within few minutes after addition of the virus solution, discrete spots appeared in the scanning image, as displayed in Figure 1B. The spots yielded nearly diffraction limited intensity profiles as shown by the cross section in Figure 1C. To verify that each spot contains the signal from a single virus, we plot the histogram of the measured intensity for 50 spots. As seen in Figure 1D, the width of the main peak is narrow enough to ensure that the great majority of the spots can be attributed to single virions. Furthermore, when we used fluorescence-labeled virus, the fluorescence and the interference images showed a complete overlap (see the Supporting Information). While individual SV40 virions resulted in an average contrast of 3.00 ± 0.87% for the scattering signal relative to the background, virus-like particles added to cover glass in identical fashion yielded on the average 1.28 ± 0.25% relative contrast (parts E−G of Figure 1). The slightly lower signal of the virus-like particles reflects their lower effective refractive index compared to intact virions due to the lack of a dense DNA−histone core. The results presented in Figure 1 clearly show the ability of the interferometric confocal microscopy to detect unlabeled individual small virions on a solid substrate with a contrast of the order of 1−3%, which is comparable to the contrast of a gold nanoparticle of 20 nm diameter.

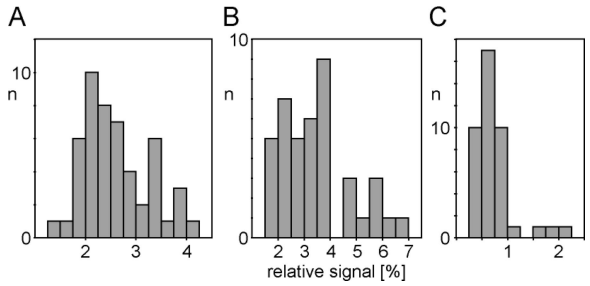


**Figure 2.** Distribution of signal intensities of the interferometric detection of particles bound to supported membrane bilayers containing 0.1 mol % GM1: (A) 20 nm colloidal gold conjugated to the cholera-toxin $\beta$ subunit; (B) SV40 virions; (C) SV40 virus-like particles.

To demonstrate the applicability of our detection technique to biologically relevant systems, we extended our experiment to visualize supported membrane bilayers. To detect scatterers bound to the membrane leaflet distal to the cover glass, we first made use of functionalized colloidal gold with a diameter of 20 nm. For specific binding, we coupled the cholera-toxin $\beta$ subunit which uses GM1 as receptor[18] to gold particles via a biotin−streptavidin coupling mechanism. Supported membrane bilayers were formed from a lipid mixture containing 0.1 mol % GM1 by the vesicle-drop method[19] on plasma-cleaned cover glass as detailed in the Supporting Information. Continuity and fluidity of the newly formed bilayers were confirmed by fluorescence recovery after photobleaching (FRAP) experiments of a membrane-incorporated fluorescent dye (Avantilipids, USA) on a confocal microscope (ZEISS LSM510) before every experiment. The bare membranes showed homogeneous background signals with few detectable impurities. Within seconds after addition of choleratoxin−gold, quantized spots appeared in the optical image with an average contrast of 2.61 ± 0.65% (Figure 2A). However, when the gold particles were functionalized with the lectin ConcanavalinA, which binds to saccharides different from the GM1 pentasaccharide, no spots appeared on GM1-containing membrane bilayers.

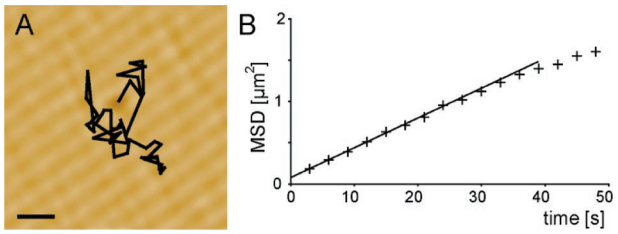


**Figure 3.** (A) Single particle tracking of an unlabeled SV40 virion bound to a supported membrane bilayer containing the viral receptor GM1 at 0.1 mol %. The trajectory is assembled from 50 frames acquired over 2.5 min. (B) Mean square displacement plot of the trajectory shown in (A). The straight slope is indicative of a diffusive motion. Scale bar is 1 $\mu$m. The background stripes correspond to a small contrast of 0.5%, which we attribute to an experimental systematic effect.

We concluded that while cholera-toxin conjugated particles bound specifically to the GM1 in the membrane bilayers and were readily detected, ConcanavalinA could not couple 20 nm gold particles to the lipid bilayers (Supporting Information). Next, we added SV40 virions (Figure 2B) and virus-like particles (Figure 2C) to membrane bilayers. Membranes were formed and virions were added as described above. We obtained a signal contrast of 3.02 $\pm$ 0.88% for SV40 virions and 0.75 $\pm$ 0.39% for SV40 virus-like particles bound to membranes.

A particularly appealing application of our detection method is in single particle tracking because the imaging technique is intrinsically photostable and due to the lack of any label ensures the unperturbed biological function of the system under study. We have explored this possibility by monitoring single virions that underwent lateral motion while they were attached to membranes. In Figure 3A we present a trace recorded from an individual SV40 virion moving in the plane of the membrane. We computationally extracted particle positions in consecutive images recorded at fixed intervals and calculated the mean square displacement and the diffusion constant following the procedure described previously.[20] As shown by an example in Figure 3B, trajectories showed linear mean square displacement plots as expected for random lateral Brownian motion. Individual virions exhibited a diffusion constant of 0.0088 $\pm$ 0.0004 $\mu$m$^2$/s. This is in agreement with our previous single fluorescent virus tracking study of the similar murine polyoma virus-like particles bound to their receptors (the glycolipid GD1a[21]) in supported membrane bilayers.[20]

By incorporating a fluorescent isoform of the SV40 receptor GM1 into the membrane bilayers, we also measured the diffusion constant of the free receptor by FRAP and found $D = 3.8 \pm 1.4$ $\mu$m$^2$/s. Thus, the free receptor is more than 2 orders of magnitude more mobile than the virion bound to it. We believe this surprising observation points to a strong virus−membrane interaction and a highly multivalent binding of the virion to its receptor. Our finding is particularly interesting because multivalent binding to lipids via antibody-coated gold has yielded only a moderate decline in $D$ in comparison with unconjugated lipid.[22] While antibodies are quite flexible, the binding sites in the virion shell are spaced in a rigid array with a separation of 32 Å.[23] Hence, viral binding is likely to impose strong structural constraints on GM1 molecules and may influence the mobility of the SV40−GM1 complex in a significant manner. We emphasize that we can rule out the contribution of the fluid-phase viscosity on the observed low diffusion constant because, as predicted by the Saffman−Delbrück model,[24] experiments on the mobility of 40 nm gold particles bound to membrane lipids[22] have reported only a minimal dependence on the aqueous phase viscosity. In addition, we also rule out photodamage to the virions or the membrane because even long-term imaging of up to 15 min did not influence binding or the random motion of the virion on the membrane. Future studies will aim at understanding the details of the interactions between SV40 and GM1 in supported membrane bilayers. Further investigations of this well-defined in vitro system composed of GM1-containing membranes and the GM1-ligand SV40 are expected to shed light on the formation of membrane microdomains in cellular membranes that lead to lipid-mediated endocytosis[14,25] and infection. This strategy is particularly promising for quantitative studies because the outcome can be directly compared with the abundant experimental data on the interaction between GM1 and the cholera-toxin $\beta$ subunit[26] using other methods.

We have shown that the detection method presented here allows label-free visualization of single virions and other nanoscopic entities in biological systems. Clearly, our label-free approach is not suited for imaging or tracking of objects in strongly scattering media such as an intact cell. Nevertheless, it holds great promise in studying the changes induced in artificial membrane bilayers by multivalent binding to GM1,[26] without introducing components such as organic dyes that might influence the bilayer. Indeed, we emphasize that weak interactions at the nanoscopic scale can have large effects[27] and that the attachment of a fluorophore does dramatically change the mobility and even the phase-preference of GM1 in model membranes.[28] In comparison with the existing techniques based on using dye molecules or semiconductor quantum dots as labels, our approach offers a few other decisive advantages. First, very long measurements can be performed on the same nanoscopic entity. In the current work, we have shown this for up to 15 min, but this is easily extendable to longer times. Second, tedious labeling chemistry can be avoided. Third, although the measurement reported here did not demand a high time resolution, our detection method is in principle capable of very fast tracking[6] because in contrast to the emission of fluorescent molecules, scattering does not saturate with light intensity. The interferometric detection is furthermore very sensitive to axial motion.[15] Finally, simultaneous label-free imaging and single molecule fluorescence detection can provide more information about the system under study. In this light, we plan to study the dynamic binding of single dye-labeled GM1 to SV40 and the three-dimensional motion of receptor-bound virions by simultaneous label-free detection of virions and single dyes attached to them.

**Acknowledgment.** The authors thank A. Oppenheim and G. Schwarzmann for generously sharing reagents and A. Renn for help with various experiments. This work was

supported by the ETH Zurich and the Swiss Ministry of Education and Science (EU Integrated Project Molecular Imaging).

**Supporting Information Available:** Experimental details, a fluorescence recovery after photobleaching control of bilayer fluidity, images of a binding control experiment, and an image of simultaneous interferometric and fluorescence detection of atto565-labeled SV40. This material is available free of charge via the Internet at http://pubs.acs.org.

## References

(1) Bräuchle, C.; Seisenberger, G.; Endress, T.; Ried, M. U.; Buning, H.; Hallek, M. *ChemPhysChem* **2002**, *3* (3), 299−303.
(2) Yildiz, A.; Forkey, J. N.; McKinney, S. A.; Ha, T.; Goldman, Y. E.; Selvin, P. R. *Science* **2003**, *300* (5628), 2061−2065.
(3) Renn, A.; Seelig, J.; Sandoghdar, V. *Mol. Phys.* **2006**, *104*, 409−414.
(4) Lindfors, K.; Kalkbrenner, T.; Stoller, P.; Sandoghdar, V. *Phys. Rev. Lett.* **2004**, *93* (3), 037401.
(5) Lasne, D.; Blab, G. A.; Berciaud, S.; Heine, M.; Groc, L.; Choquet, D.; Cognet, L.; Lounis, B. *Biophys. J.* **2006**, *91* (12), 4598−4604.
(6) Jacobsen, V.; Stoller, P.; Brunner, C.; Vogel, V.; Sandoghdar, V. *Opt. Express* **2006**, *14* (1), 405−414.
(7) Boyer, D.; Tamarat, P.; Maali, A.; Lounis, B.; Orrit, M. *Science* **2002**, *297* (5584), 1160−1163.
(8) Arbouet, A.; Christofilos, D.; Del Fatti, N.; Vallee, F.; Huntzinger, J. R.; Arnaud, L.; Billaud, P.; Broyer, M. *Phys. Rev. Lett.* **2004**, *93* (12), 127401.
(9) Ignatovich, F. V.; Novotny, L. *Phys. Rev. Lett.* **2006**, *96* (1), 013901.
(10) Brehm, M.; Taubner, T.; Hillenbrand, R.; Keilmann, F. *Nano Lett.* **2006**, *6* (7), 1307−10.
(11) Liddington, R. C.; Yan, Y.; Moulai, J.; Sahli, R.; Benjamin, T. L.; Harrison, S. C. *Nature* **1991**, *354* (6351), 278−284.
(12) Tsai, B.; Gilbert, J. M.; Stehle, T.; Lencer, W.; Benjamin, T. L.; Rapoport, T. A. *EMBO J.* **2003**, *22* (17), 4346−4355.
(13) Pelkmans, L.; Puntener, D.; Helenius, A. *Science* **2002**, *296* (5567), 535−539.
(14) Pelkmans, L.; Kartenbeck, J.; Helenius, A. *Nat. Cell Biol.* **2001**, *3* (5), 473−483.
(15) Jacobsen, V.; Klotzsch, E.; Sandoghdar, V., Interferometric detection and tracking of nanoparticles. In *Nano Biophotonics*, Masuhara, H., Kawata, S., Tokunaga, F., Eds.; Elsevier: Amsterdam, 2007; Vol. 3, pp 143−159.
(16) Vörös, J. *Biophys. J.* **2004**, *87* (1), 553−561.
(17) Sandalon, Z.; Oppenheim, A. *Virology* **1997**, *237* (2), 414−421.
(18) Holmgren, J.; Lonnroth, I.; Mansson, J.; Svennerholm, L. *Proc. Natl. Acad. Sci. U.S.A.* **1975**, *72* (7), 2520−2524.
(19) Kalb, E.; Frey, S.; Tamm, L. K. *Biochim. Biophys. Acta* **1992**, *1103* (2), 307−316.
(20) Ewers, H.; Smith, A. E.; Sbalzarini, I. F.; Lilie, H.; Koumoutsakos, P.; Helenius, A. *Proc. Natl. Acad. Sci. U.S.A.* **2005**, *102* (42), 15110−15115.
(21) Smith, A. E.; Lilie, H.; Helenius, A. *FEBS Lett.* **2003**, *555* (2), 199−203.
(22) Lee, G. M.; Ishihara, A.; Jacobson, K. A. *Proc. Natl. Acad. Sci. U.S.A.* **1991**, *88* (14), 6274−6278.
(23) Stehle, T.; Gamblin, S. J.; Yan, Y.; Harrison, S. C. *Structure* **1996**, *4* (2), 165−182.
(24) Saffman, P. G.; Delbruck, M. *Proc. Natl. Acad. Sci. U.S.A.* **1975**, *72* (8), 3111−3113.
(25) Chinnapen, D. J.; Chinnapen, H.; Saslowsky, D.; Lencer, W. I. *FEMS Microbiol. Lett.* **2006**.
(26) Forstner, M. B.; Yee, C. K.; Parikh, A. N.; Groves, J. T. *J. Am. Chem. Soc.* **2006**, *128* (47), 15221−15227.
(27) Coleman, P. *Nature* **2007**, *446* (7134), 379.
(28) Burns, A. R.; Frankel, D. J.; Buranda, T. *Biophys. J.* **2005**, *89* (2), 1081−1093.

NL070766Y